Energy Conversion and Management 51 (2010) 1148–1156

Contents lists available at ScienceDirect

Energy Conversion and Management

journal homepage: www.elsevier.com/locate/enconman

Practical viewpoints on load frequency control problem in a deregulated power system

Elyas Rakhshani [a,*], Javad Sadeh [b]

[a] Islamic Azad University, Gonabad Branch, Gonabad, Iran
[b] Electrical Engineering Department, Faculty of Engineering, Ferdowsi University of Mashhad, Mashhad, Iran

ARTICLE INFO

Article history:
Received 4 December 2009
Accepted 13 December 2009
Available online 18 January 2010

Keywords:
Load frequency control
Deregulated power system
Optimal output feedback
Reduced-order observer

ABSTRACT

An attempt is made in this paper to present feasible and practical methods to improve dynamic response of load frequency control problem in a deregulated power system. In the practical environment, access to all of the state variables of system is limited and measuring all of them is also impossible. Access and also measuring the state variable is one of the most problems on application of control methods in real world. To solve this problem, in this paper, two methods with pragmatic viewpoint are proposed. The first method is optimal output feedback control and the second is based on state observer method. In the output feedback method, only the measurable state variables within each control area are required to use for feedback. But when we have fewer sensors available than the number of states or it may be undesirable, expensive, or impossible to directly measure all of the states, using a reduced-order observer is proposed. These proposed designs, which are presented in this paper, have been developed in order to over-come this problem and are tested on a two-area power system considering different contracted scenarios. The results show that when the power demands change, the output feedback method is the most rational technique with the best dynamic response. Also, with using a reduced-order observer, the dynamic response of system is improved. In fact, using these methods is necessary for load frequency control problem in a practical environment.

1. Introduction

Investigation of the power system markets shows that frequency control is one of the most profitable ancillary services at these systems. The basic theory of LFC is much consolidated and well known [1–3]. But with the restructuring of electric markets, Load Frequency Control requirements should be expanded to include the planning functions necessary to insure the resources needed for LFC implementation. Thus, the LFC system keeps track of the momentary active power imbalance, detects it, corrects it and communicates an adequate amount of the balance energy service basis, to the market operating system. A lot of studies have been made about LFC in a deregulated environment [4]. These studies try to modify the conventional LFC system to take into account the effect of bilateral contracts on the dynamics and continued with proposed model in [5]. After that more researches are done to improve the dynamical response of system under competitive conditions [6]. The conventional control strategy for the LFC problem is to take the integral of the area control error (ACE) as the control signal. An integral controller provides zero steady state deviation, but it exhibits poor dynamic performance. To improve the transient response, various control strategies, such as linear feedback, optimal control and Kalman estimator method, have been proposed [6,7]. However, these methods are idealistic or need some information of the system states, which are very difficult to know completely.

There have been continuing efforts in designing LFC with better performance using intelligence algorithms [8] or robust methods [9,10]. These methods show good dynamical responses, but some of them suggest complex and or high order dynamical controllers [10], which are not practical for industry practices yet.

In this paper, the dynamical response of the load frequency control problem in the deregulated environment is improved with a pragmatic viewpoint. Because in the practical environment (real world), access to all of the state variables of system is limited and the measuring all of them is impossible. So some of these states should be estimated or neglected for feedback. To solve this problem, in this paper, two methods are proposed. The first method is the optimal output feedback control and the second is based on state observer method. In the output feedback method, by selecting desired output matrix (C), un-measurable states are

* Corresponding author. Address: Vakil Abad Bolv., Sayad Shirazi 27, No. 2, Postal Code: 91799-99497, Mashhad, Iran. Mobile: +98 915 322 7131; fax: +98 511 8763302.
E-mail addresses: Elyas.rakhshani@gmail.com (E. Rakhshani), Sadeh@um.ac.ir (J. Sadeh).

0196-8904/$ - see front matter © 2009 Elsevier Ltd. All rights reserved.
doi:10.1016/j.enconman.2009.12.024

Nomenclature

f	frequency	AGPM	Augmented Generation Participation Matrix
B	frequency bias	K_P	power system equivalent gain
R	droop characteristic	T_P	power system equivalent time constant
u	input vector	T_G	time constant of governor
x	state vector	T_T	time constant of turbine
ζ	deviation of scheduled tie-line power flow	T_{T-G}	augmented time constant of turbine–governor set
K_{i}	integration controller gain	d	total demand
AGC	automatic generation control	ΔP_{Loc}	total local contracted demand
LFC	load frequency control	ΔP_M	power generation of GENCO
GENCO	Generation company	ΔP_L	contracted demand of DISCO
DISCO	Distribution company	ΔP_{UL}	un-contracted demand
ISO	independent system operator	ΔP_d	area load disturbance
VIU	vertically integrated utility	T_{12}	tie-line synchronizing coefficient between areas
TRANSCO	Transmission company	ΔP_{tie}	net tie-line power flow
ACE	area control error	$\Delta P_{\mathrm{tie,error}}$	tie-line power error
apf	area participation factor	$\Delta P_{\mathrm{tie,actual}}$	tie-line actual power
gpf	generator participation factor		

neglected for feedback, so only the measurable state variables in output within each control area are required to use for feedback. But in the second method, un-measurable states are estimated using a reduced-order observer method. These proposed methods are tested on a two-area power system considering different contracted scenarios. The results of proposed controllers are separately compared with full-state and full-order observer methods. The results show that when the power demands change, the output feedback method is the most rational technique with the best response. Also, with using a reduced-order observer, the dynamic response of the system is improved. In fact, using these methods is necessary for LFC problem in a practical environment.

2. Multi-area LFC in a deregulated environment

In the competitive environment of power system, the vertically integrated utility (VIU) no longer exists. Deregulated system will consist of GENCOs, DISCOs, transmission companies (TRANSCOs) and independent system operator (ISO). However, the common AGC goals still remain. In the system, any GENCO in any area may supply both DISCOs in its user pool and DISCOs in other areas through tie-lines between areas. In another words, for restructured system having several GENCOs and DISCOs, any DISCO may contract with any GENCO in another control area independently. This case is called as 'bilateral transactions'. The transactions have to be implemented through an independent system operator. The impartial entity, ISO, has to control many ancillary services, one of which is AGC. In deregulated environment, any DISCO has the liberty to buy power at competitive prices from different GENCOs, which may or may not have contract in the same area as the DISCO. This section gives a brief overview of this generalized model that uses all the information required in a VIU industry plus the contract data information. Based on the idea presented in [9], the concept of an 'Augmented Generation Participation Matrix' (AGPM) to express the possible contracts following is presented here. The AGPM shows the participation factor of a GENCO in the load following contract with a DISCO. The number of rows and columns of AGPM matrix is equal to the total number of GENCOs and DISCOs in the overall power system, respectively. So, the AGPM structure for a large-scale power system with N control areas is given by

$$\mathrm{AGPM} = \begin{bmatrix} \mathrm{AGPM}_{11} & \cdots & \mathrm{AGPM}_{1N} \\ \vdots & \ddots & \vdots \\ \mathrm{AGPM}_{N1} & \cdots & \mathrm{AGPM}_{NN} \end{bmatrix},$$

where

$$\mathrm{AGPM}_{ij} = \begin{bmatrix} gpf_{(s_i+1)(z_j+1)} & \cdots & gpf_{(s_j+1)(z_j+m_j)} \\ \vdots & \ddots & \vdots \\ gpf_{(s_i+n_j)(z_j+1)} & \vdots & gpf_{(s_j+n_i)(z_j+m_j)} \end{bmatrix},$$
$$\text{for } i,j = 1,\ldots,N \quad \text{and}$$
$$s_i = \sum_{k=1}^{i-1} n_i,\ \ z_j = \sum_{k=1}^{i-1} m_j,\ \ s_1 = z_1 = 0.$$

In the above, n_i and m_i are the number of GENCOs and DISCOs in area i and gpf_{ij} refers to 'generation participation factor' and shows the participation factor of GENCO$_i$ in the total load following requirement of DISCO$_j$ based on the possible contract. The sum of all entries in each column of an AGPM is unity. The diagonal sub-matrices of AGPM correspond to local demands and off-diagonal sub-matrices correspond to demands of DISCOs in one area on GENCOs in another area. The details and block diagram of the generalized AGC scheme for a two-area deregulated power system are shown in Fig. 1. Dashed lines show interfaces between areas and the demand signals based on the possible contracts. These new information signals are absent in the traditional LFC scheme. As there are many GENCOs in each area, the ACE signal has to be distributed among them due to their ACE participation factor in the LFC task and $\sum_{j=1}^{n_i} apf_{ji} = 1$. We can write [9]:

$$d_i = \Delta P_{Loc,i} + \Delta P_{di} \tag{1}$$

where

$$\Delta P_{Loc,i} = \sum_{j=1}^{m_i} \Delta P_{Lj-i}, \quad \Delta P_{di} = \sum_{j=1}^{m_i} \Delta P_{ULj-i} \tag{2}$$

$$\zeta_i = \sum_{\substack{k=1 \\ k\neq 1}}^{N} \Delta P_{tie,ik,scheduled} \tag{3}$$

$$\eta_i = \sum_{\substack{j=1 \\ j\neq 1}}^{N} T_{ij}.\Delta f_j \tag{4}$$

$$\Delta P_{tie,ik,scheduled} = \sum_{j=1}^{n_i} \sum_{t=1}^{m_k} apf_{(s_i+j)(z_k+t)} \Delta P_{Lt-k} - \sum_{t=1}^{n_k} \sum_{j=1}^{m_i} apf_{(s_k+t)(z_i+j)} \Delta P_{Lj-i} \tag{5}$$

$$\Delta P_{tie,i,error} = \Delta P_{tie,i,actual} - \zeta_i \tag{6}$$

$$\Delta P_{m,k-i} = \rho_{ki} + apf_{ki} \sum_{j=1}^{m_i} \Delta P_{ULj-i} \quad k = 1,2,\ldots,n_i \tag{7}$$

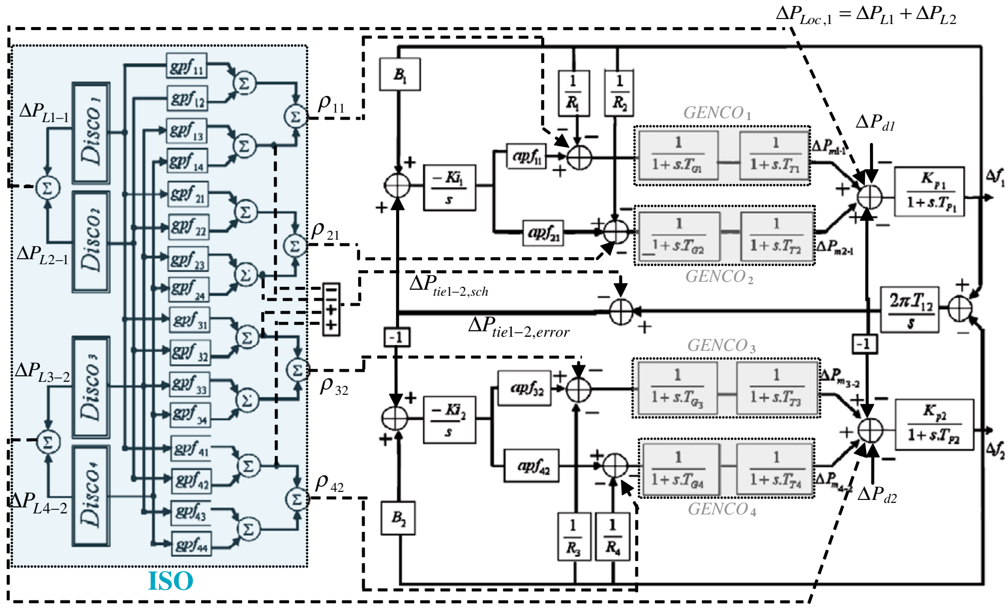

Fig. 1. Modified LFC system in a deregulated environment for this study.

$$\rho_{ki} = \sum_{j=1}^{N} \left[\sum_{t=1}^{m_j} gpf_{(s_i+k)(z_j+t)} \Delta P_{Lt-j} \right] \tag{8}$$

Also the error signal in (6) is used to generate its ACE signals in the steady state as follows:

$$\mathrm{ACE}_i = B_i \Delta f_i + \Delta P_{tie,i,error} \tag{9}$$

To illustrate the effectiveness of the modeling strategy and proposed control design, a two control area power system is considered as a test system. It is assumed that each control area includes two GENCOs and DISCOs as shown in Fig. 2. So the closed-loop system in Fig. 1 is characterized in state space form as follows:

$$\dot{x} = A \cdot x + B \cdot u, \quad x(t_0) = x_0 \tag{10}$$

$$y = C \cdot x \tag{11}$$

A fully controllable and observable model for a two-area power system is proposed, where x is the state vector and u is the vector of power demands of the DISCOs.

$$u = [\Delta P_{L1-1} \quad \Delta P_{L2-1} \quad \Delta P_{L3-2} \quad \Delta P_{L4-2} \quad \Delta P_{d1} \quad \Delta P_{d2}]^T \tag{12}$$

$$x = \left[\Delta f_1 \ \ \Delta f_2 \ \ \Delta P_{m1-1} \ \ \Delta P_{m2-1} \ \ \Delta P_{m3-2} \ \ \Delta P_{m4-2} \ \ \textstyle\int \mathrm{ACE}_1 \ \ \int \mathrm{ACE}_2 \ \ \Delta P_{tie1-2,actual}\right]^T \tag{13}$$

The deviation of frequency, turbine output and tie-line power flow within each control area are measurable outputs, other states such as: governor outputs, integration of ACE are not measurable so one of the presented methods in Section 3, will be used to over-come this problem. Note that the used LFC system in this paper is a modified system of the proposed model in [5]. The proposed model in [5] is not fully controlable so as shown in Fig. 1, it is assumed that:

$$\boxed{\mathbf{GENCO}} \equiv \boxed{\frac{1}{1+sT_{T-G}}} \quad \text{and} \quad T_{T-G} = T_G + T_T$$

where T_{T-G} is the augmented time constant of turbine–generator set in Fig. 1. As shown in Fig. 1, (dotted lines around the turbines and governors blocks), in this proposed model, the outputs of governors are neglected to access a fully controllable and observable system.

3. Controller design

In this paper to improve the dynamical response of system with a pragmatic viewpoint, two control strategies, optimal output feedback and reduced-order observer control are proposed. Brief theories of these methods are described in this section [11,12]:

3.1. Optimal output feedback control

For the system that is defined by Eqs. (10) and (11), output feedback control law is:

$$u = -K \cdot y \tag{14}$$

The objective of this regulator for the system may be attained by minimizing a performance index (J) of the type:

$$J = 1/2 \int [x^T(t) \cdot Q \cdot x(t) + u^T(t) \cdot R \cdot u(t)]dt \tag{15}$$

or

$$J = 1/2 \int x^T (Q + C^T K^T RKC) x \, dt \tag{16}$$

By substituting Eq. (14) into (10), the closed-loop system equations are found to be:

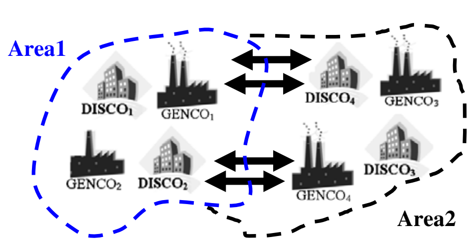

Fig. 2. An example for configuration of the power system.

$$\dot{x} = (A - BKC)x = A_c x \tag{17}$$

This dynamical optimization may be converted to an equivalent static one that is easier to solve as follows. So a constant, symmetric, positive-semidefinite matrix P can be defined as:

$$d(x^T P x)/dt = -x^T(Q + C^T K^T RKC)x \tag{18}$$

$$J = 1/2 \cdot x^T(0)Px(0) - 1/2 \lim_{t\to\infty} x^T(t)P \cdot x(t) \tag{19}$$

Assuming that the closed-loop system is stable so that $x(t)$ vanishes with time, this becomes:

$$J = 1/2 \cdot x^T(0)Px(0) \tag{20}$$

If P satisfies (18), then we may use (17) to see that:

$$\begin{aligned} -x^T(Q + C^T K^T RKC)x &= d(x^T P x)/dt = \dot{x}^T P x + x^T P \dot{x} \\ &= x^T\left(A_c^T P + PA_c\right)x \end{aligned} \tag{21}$$

$$g \equiv A_c^T P + PA_c + C^T K^T RKC + Q = 0 \tag{22}$$

We may write (20) as:

$$J = 1/2 \cdot tr(PX) \tag{23}$$

where the $n \times n$ symmetric matrix X is defined as:

$$X = E\{x(0) \cdot x^T(0)\} \tag{24}$$

So the best K should be selected, to minimize (16) subject to the constraint (22) on the auxiliary matrix P. To solve this modified problem, Lagrange multiplier approach will be used and the constraint will be adjoined by defining this Hamiltonian:

$$H = tr(PX) + tr(gS) \tag{25}$$

Now to minimize (23), partial derivatives of H with respect to all the independent variables P, S and K should be equal to zero

$$0 = \frac{\partial H}{\partial S} = A_c^T P + PA_c + C^T K^T RKC + Q \tag{26}$$

$$0 = \frac{\partial H}{\partial P} = A_c S + SA_c^T + X \tag{27}$$

$$0 = 1/2 \cdot (\partial H/\partial K) = RKCSC^T - B^T PSC^T \tag{28}$$

To obtain the output feedback gain K with minimizing (16), these three coupled Eqs. (26)–(28) should be solved simultaneously. The first two of these are Lyapunov equations and the third is an equation for the gain K. If R is positive definite and is nonsingular, then (28) may be solved for K [11]:

$$K = R^{-1} B^T PSC^T (CSC^T)^{-1} \tag{29}$$

To solve these equations, an iterative algorithm is presented in Appendix A.

3.2. Reduced-order observer control

In practical environments only some of the state variables are measurable. These are defined as output variables such as:

$$y_{p\times 1} = C_{p\times n} \cdot x_{n\times 1}, \quad p < n \tag{30}$$

The interesting case is when we have less sensors available (p) than the number of states (n), $p < n$. suppose we can measure some of the state variables contained in x, and the state vector x is partitioned into two sets,

x_1: variables that can be measured directly,
x_2: variables that cannot be measured directly.

$$\begin{cases} \dot{x}_1 = A_{11} \cdot x_1 + A_{12} \cdot x_2 + B_1.u \\ \dot{x}_2 = A_{21} \cdot x_1 + A_{22} \cdot x_2 + B_2 \cdot u \end{cases} \tag{31}$$

and the observation equation is:

$$y = C_1 \cdot x_1 \tag{32}$$

where C_1 is square and nonsingular matrix. The full-order observer for the states is then:

$$\begin{cases} \dot{\hat{x}}_1 = A_{11} \cdot \hat{x}_1 + A_{12} \cdot \hat{x}_2 + B_1 \cdot u + L_1 \cdot (y - C_1 \cdot \hat{x}_1) \\ \dot{\hat{x}}_2 = A_{21} \cdot \hat{x}_1 + A_{22} \cdot \hat{x}_2 + B_2 \cdot u + L_2 \cdot (y - C_1 \cdot \hat{x}_1) \end{cases} \tag{33}$$

But we do not need to solve first observer equation for x_1 because these states can be solved directly using (32):

$$\hat{x}_1 = x_1 = C_1^{-1} \cdot y \tag{34}$$

In this case the observer for those states that cannot be measured directly is designed as follows:

$$\dot{\hat{x}}_2 = A_{21} \cdot C_1^{-1} \cdot y + A_{22} \cdot \hat{x}_2 + B_2 \cdot u \tag{35}$$

The block diagram of this reduced-order observer is shown in Fig. 3.

This is a dynamic system of the same order as the number of state variables that cannot be measured directly. The dynamic behavior of this reduced-order observer is governed by the eigenvalues of A_{22}, a matrix over which the designer has no control. Since there is no assurance that the eigenvalues of A_{22} are suitable, we need a more general system for the reconstruction of x_2. We take:

$$\hat{x}_2 = L \cdot y + z \tag{36}$$

where

$$\dot{z} = F \cdot z + G \cdot y + H \cdot u \tag{37}$$

Define the estimation error as follows:

$$e = x - \hat{x} = \begin{bmatrix} x_1 - \hat{x}_1 \\ x_2 - \hat{x}_2 \end{bmatrix} = \begin{bmatrix} e_1 \\ e_2 \end{bmatrix} = \begin{bmatrix} 0 \\ e_2 \end{bmatrix} \tag{38}$$

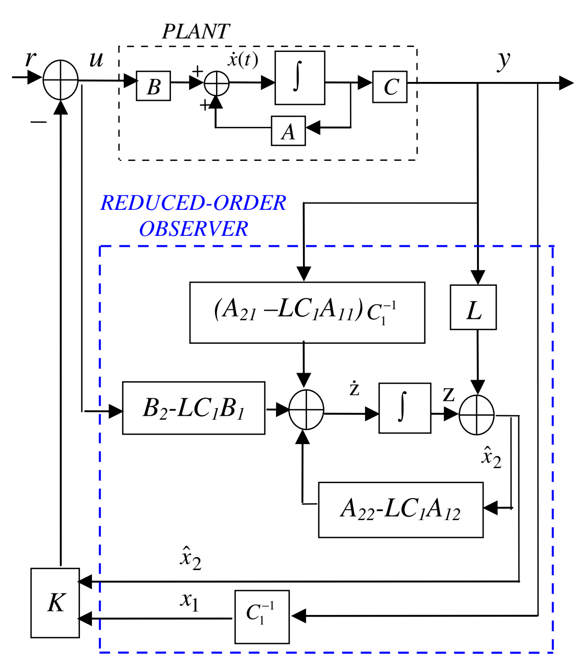

Fig. 3. Block diagram of reduced-order observer.

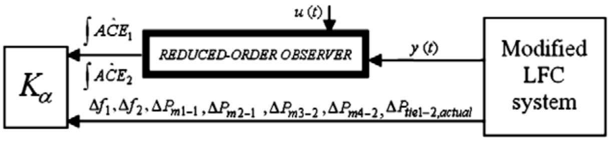

Fig. 4. Schematic diagram of applied reduced-order observer.

and we get:

$$\begin{aligned}\dot{e}_2 &= \dot{x}_2 - \dot{\hat{x}}_2 = A_{21}\cdot x_1 + A_{22}\cdot x_2 + B_2\cdot u - L\cdot\dot{y} - \dot{z}\\ &= A_{21}\cdot x_1 + A_{22}\cdot x_2 + B_2\cdot u - LC_1\cdot\dot{x}_1 - F\cdot z - G\cdot y - H\cdot u\\ &= A_{21}\cdot x_1 + A_{22}\cdot x_2 + B_2\cdot u - LC_1(A_{11}\cdot x_1 + A_{12}\cdot x_2 + B_1\cdot u)\\ &\quad - F(\hat{x}_2 - L\cdot y) - G\cdot y - H\cdot u \end{aligned} \tag{39}$$

Since:

$$\hat{x}_2 - L\cdot y = x_2 - e_2 - L\cdot y = x_2 - e_2 - LC_1\cdot x_1 \tag{40}$$

we get:

$$\begin{aligned}\dot{e}_2 &= Fe_2 + (A_{21} - LC_1A_{11} - GC_1 + FLC_1)x_1\\ &\quad + (A_{22} - LC_1A_{12} - F)\cdot x_2 + (B_2 - LC_1B_1 - H)u\end{aligned} \tag{41}$$

In order for the error to be independent of x_1, x_2, and u, the matrices multiplying x_1, x_2, and u must vanish:

$$\begin{cases} F = A_{22} - LC_1A_{12}\\ H = B_2 - LC_1B_1\\ G = (A_{21} - LC_1A_{11})C_1^{-1} + FL\end{cases} \tag{42}$$

Then:

$$\dot{e}_2 = F\cdot e_2 \tag{43}$$

And for stability of the observer dynamic system, the eigenvalues of F must lie in the left hand-side of s plane. Therefore, we see that the problem of reduced-order observer is similar to the full-order observer with $(A_{22} - LC_1A_{12})$ playing the role of $(A - LC)$.

Based on the information of system in Section 2, the integration of ACE *is* not a measurable state and as shown in Fig. 4, should be estimated by a reduced-order observer.

4. Simulation results

In this section, to verify the performance of proposed methods, two separate studies are presented.

The first one is based on neglecting the un-measurable states for feedback using optimal output feedback control considering one scenario of possible contracts under practical operating conditions and large load demands (scenarios 1). In fact by selecting the desired output matrix (C), presented in Appendix C, un-measurable states are neglected and only the measurable state variables in output within each control area are required to use for feedback.

The second study is based on estimation of un-measurable states using reduced-order observer method (scenario 2). For performance comparison in each study, the full-state feedback and full-order observer control are also simulated and the results are presented, separately. The simulations are done using MATLAB platform [13] and the power system parameters with state space matrixes are given in Appendix. Note that, in the presented scenarios there is not any especial comparison between these two methods and the main objective of this paper is to present and design two practical controllers for LFC case.

4.1. Scenario 1: transaction based on free contracts with optimal output feedback control

In this scenario, it is considered that each DISCO demands 0.1 pu MW total power from GENCOs as defined by entries in AGPM and each GENCO participates in ACE as defined by following *apfs*:

$$\begin{aligned}&apf_{1-1} = 0.75,\quad apf_{2-1} = 1 - apf_{1-1} = 0.25\\ &apf_{3-2} = 0.5,\quad apf_{4-2} = 1 - apf_{3-2} = 0.5\end{aligned}$$

Also it is assumed that DISCOs have the freedom to have a contract with any GENCO in their or other areas. These contracts can be shown in following AGPM:

$$\text{AGPM} = \begin{bmatrix} 0.5 & 0.25 & 0 & 0.3\\ 0.2 & 0.25 & 0 & 0\\ 0 & 0.25 & 1 & 0.7\\ 0.3 & 0.25 & 0 & 0\end{bmatrix}$$

Performance index of optimal output feedback method for the first study is given in Fig. 5 and the simulation results for the first scenario are shown in Figs. 6–8.

As shown in Fig. 6, in the steady state, any GENCO generation must match the demand of the DISCOs in contract with it, according to (7):

$$\begin{aligned}&\Delta P_{m1-1} = 0.105\ \text{pu MW},\quad \Delta P_{m2-1} = 0.045\ \text{pu MW}\\ &\Delta P_{m3-2} = 0.195\ \text{pu MW},\quad \Delta P_{m4-2} = 0.055\ \text{pu MW}\end{aligned}$$

Based on simulation results shown in Figs 7 and 8a, the effectiveness of optimal output feedback method can be observed especially by comparison with a system without any controller.

Note that by selecting matrix C, the number of state variables used in output feedback is less that the number of those in full-state feedback, because in output feedback only measurable states are used. Considering this fact, the dynamic responses of frequency in each area and the tie-line power flow is also acceptable compared with full-state feedback.

The off-diagonal blocks of the AGPM correspond to the contract of a DISCO in one area with a GENCO in another area. As shown in Fig. 8a, the tie-line power flow properly converges to the specified value of (5) in the steady state, i.e. $\Delta P_{tie1-2,scheduled} = -0.05$ pu.

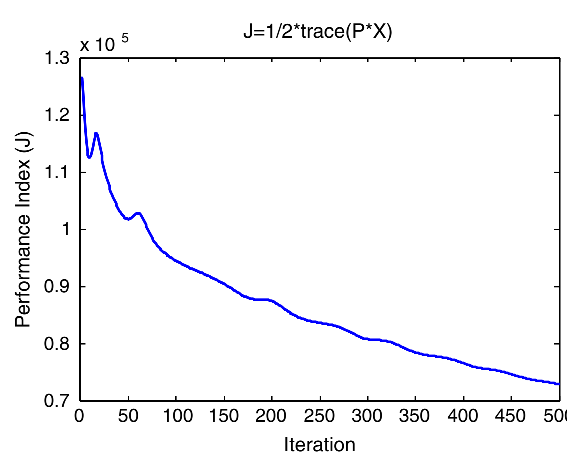

Fig. 5. Performance index for the optimal output feedback.

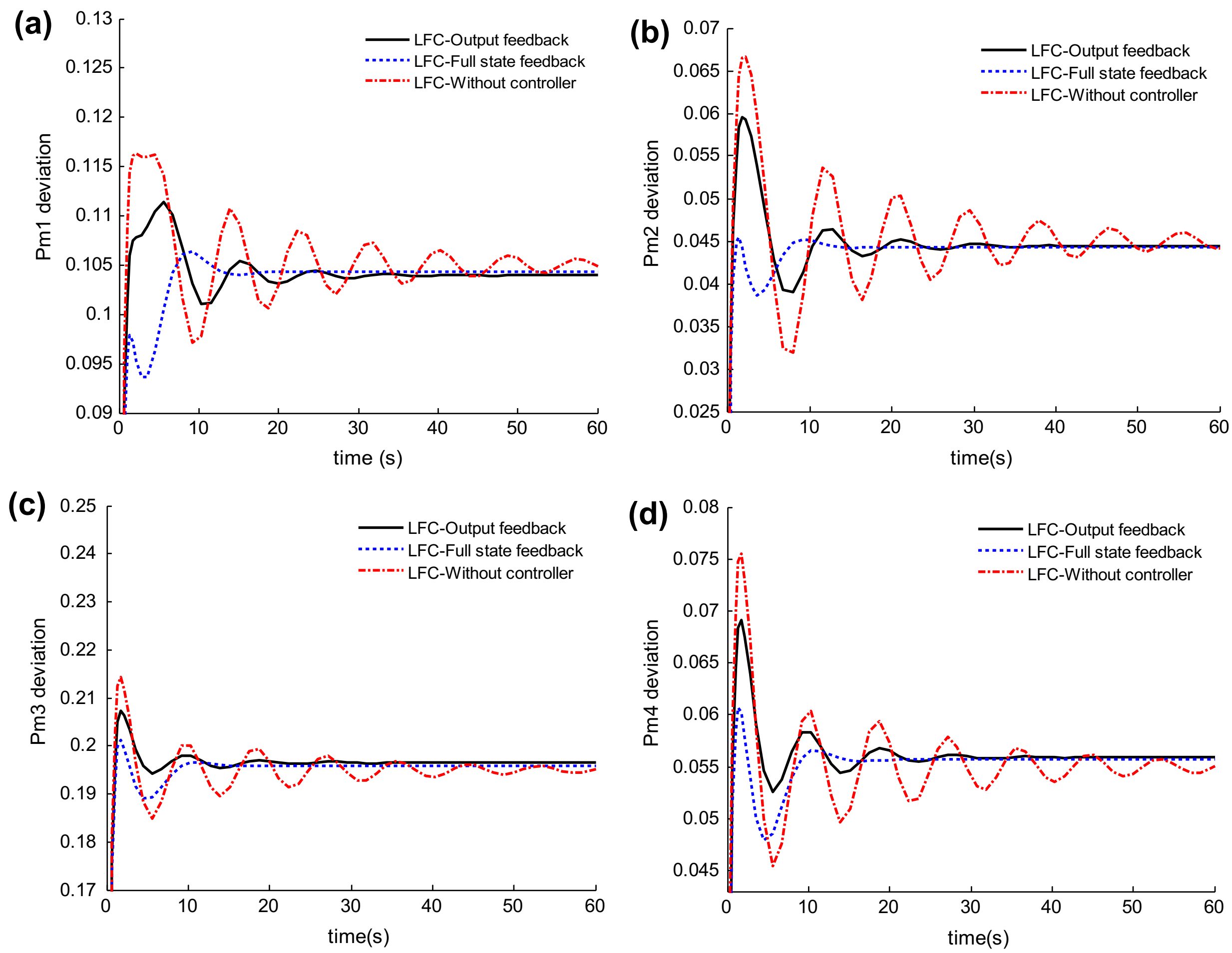

Fig. 6. a–d are the deviation of turbine power (pu MW) of the GENCO1 to GENCO4 (scenario 1).

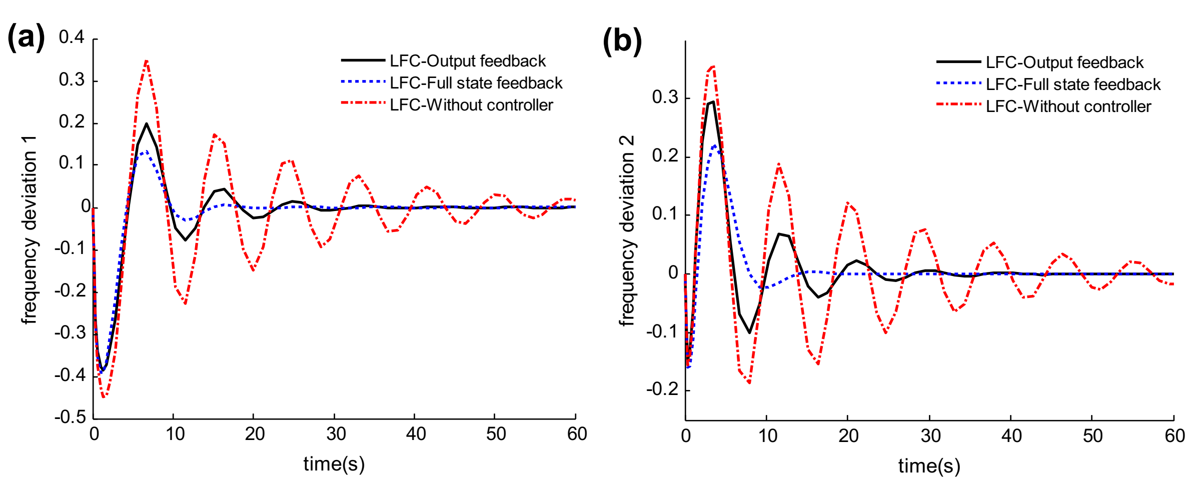

Fig. 7. (a) Frequency deviation in area 1 (rad/s) and (b) frequency deviation in area 2 (rad/s) (scenario 1).

4.2. Scenario 2: transaction based on free contracts and no violation with reduced-order observer control

In order to improve the performance of LFC system, in this scenario, a reduced-order observer is designed and used for state feedback control. In this scenario, AGPM is assumed to be as follows:

$$\mathrm{AGPM} = \begin{bmatrix} 0.5 & 0.25 & 0 & 0.3 \\ 0 & 0 & 0 & 0 \\ 0 & 0.5 & 1 & 0.7 \\ 0.5 & 0.25 & 0 & 0 \end{bmatrix}$$

Based on this AGPM, $GENCO_2$ does not have any contract with other DISCOs. It is assumed that all of the changes in load de-

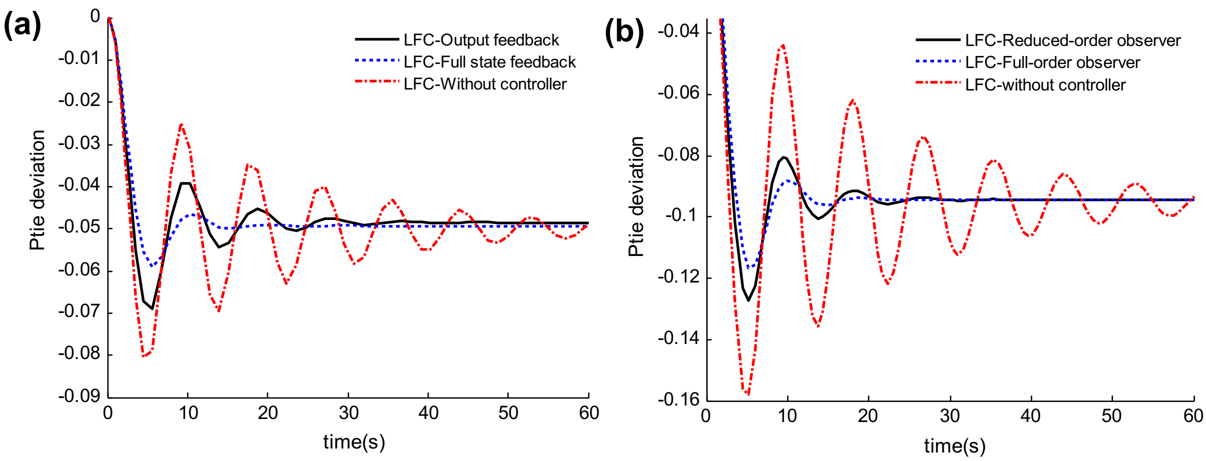

Fig. 8. Deviation of tie-line power flow (pu MW): (a) scenario1 and (b) scenario 2.

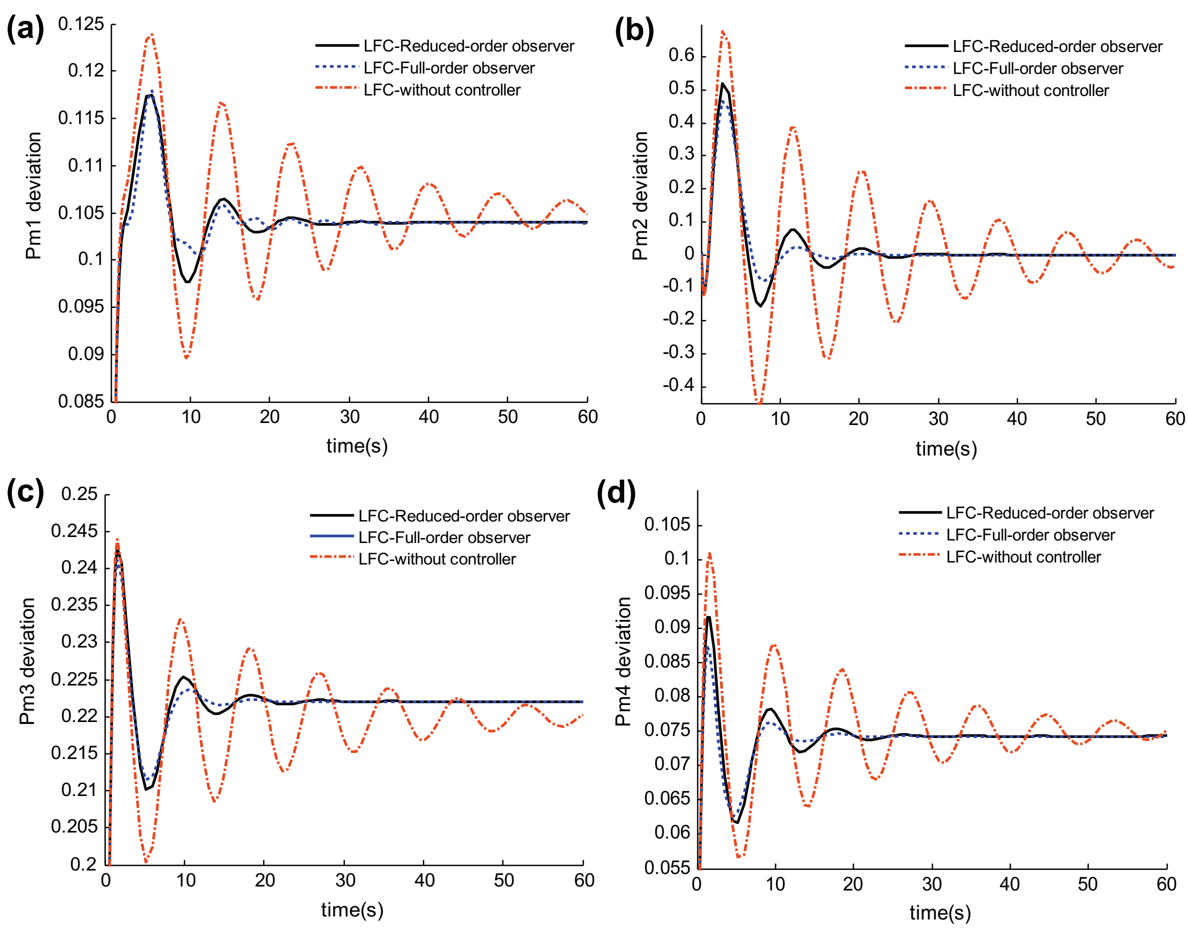

Fig. 9. a–d are the deviation of turbine power (pu MW) of the $GENCO_1$–$GENCO_4$ (scenario 2).

mands occur in bilateral contract and there is not any violation of contracted demands. Also, it is assumed that each DISCO demands 0.1 pu MW total power from other GENCOs as defined by entries in AGPM, and GENCOs participations in ACE are defined as follow:

$$apf_{1-1} = 0.75, \quad apf_{2-1} = 1 - apf_{1-1} = 0.25$$
$$apf_{3-2} = 0.5, \quad apf_{4-2} = 1 - apf_{3-2} = 0.5$$

The results for this scenario are given in Figs. 8b–10. As shown in Fig. 8b, the tie-line power flow properly converges to the specified value of (5) in the steady state, i.e. $\Delta P_{tie1-2,scheduled} = -0.095$ pu MW.

The turbine power of GENCOs and frequency deviations are shown in Figs. 9 and 10, respectively. In these figures, the performance of the reduced-order observer is compared with the full-order observer.

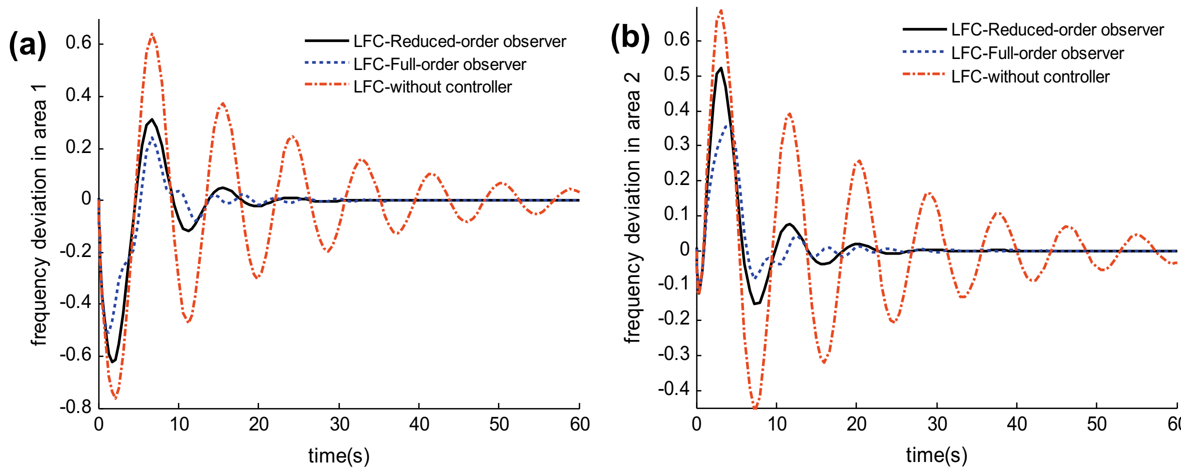

Fig. 10. (a) Frequency deviation in area 1 (rad/s) and (b) frequency deviation in area 2 (rad/s). (scenario 2).

Based on simulation results in Fig. 9 and according to (7), the actual generated powers of the GENCOs, properly converge to the desired value in the steady state. That is,

$$\Delta P_{m1-1} = 0.5(0.1) + 0.25(0.1) + 0 + 0.3(0.1) = 0.105 \text{ pu MW}$$
$$\Delta P_{m2-1} = 0.0 \text{ pu MW}$$
$$\Delta P_{m3-2} = 0.22 \text{ pu MW}$$
$$\Delta P_{m4-2} = 0.075 \text{ pu MW}$$

It is clear that, with using this method, the frequency deviation of each area, the tie-line power flow and generated power deviation have a good dynamic response in comparing with initial system without controller.

Note that we could make the observer error decay as rapidly as we wished by putting the observer poles sufficiently far into the left hand-side of the $j\omega$-axis. The observer should be slightly faster than the process (system) so that the error vanishes after a short time period.

5. Conclusion

In this paper, two practical approaches based on optimal control have been presented and applied to modified multi-area LFC after deregulation.

Modified LFC after deregulation is an important issue in power systems. In research of LFC problem, a special attention should be given to the load frequency control requirements in a practical environment, and the ability of the used controller in tracking the load changes under market conditions and should consider that some of the state variables are not accessible for measuring in a large power system. So, with a pragmatic viewpoint, two methods, i.e. optimal output feedback control and reduced-order observer methods are presented to satisfy all of these requirements.

The performance of the proposed methods is evaluated on a two-area power system with different contracted scenarios. The results of the proposed controller are also compared with the full-state feedback and full-order observer methods, separately. The simulation results show that proposed strategies are very effective and guarantees good performance. In fact, these methods provide a control system that satisfies the load frequency control requirements and with a credible dynamic response.

Appendix A. Algoritms

The algorithm which is used for solving optimal output feedback gain matrix is described as follows [11]:

1. *Initialize*:
   Set $k = 0$
   Determine a gain K_0 so that $A - BK_0C$ is asymptotically stable.
2. *kth iteration*:
   Set $A_k = A - BK_k C$
   Solve for P_k and S_k in
   $0 = A_k^T P_k + P_k A_k + C^T K_k^T R K_k C + Q$
   $0 = A_k S_k + S_k A_k^T + X$
   Set $J_k = tr(P_k X)$
   Evaluate the gain update direction
   $\Delta K = R^{-1} B^T P S C^T (C S C^T)^{-1} - K_k$
   $K_{k+1} = K_k + \alpha \Delta K$
   where α is chosen so that $A - BK_{k+1}C$ is asymptotically stable and:
   $J_{k+1} = 1/2 tr(P_{k+1} X) \leqslant J_k$
   If J_{k+1} and J_k are close enough to each other, go to 3 Otherwise, set $k = k + 1$ and go to 2
3. *Terminate*:
   Set $K = K_{k+1}$, $J = J_{k+1}$ Stop.

Appendix B. Parameters of power system

The parameter values of the power system are given in Table 1.

Appendix C. State space matrix (*A*, *B* and *C*)

In this paper, the state matrix (A), the input matrix (B) and the output matrix (C) of the proposed LFC model are as follow, where the controllability and observability matrices are full rank.

Table 1
Parameters value of power system.

GENCOs parameters (k in area i)	Area 1		Area 2	
	1-1	2-1	1-2	2-2
T_T (s)	0.4	0.375	0.375	0.4
T_G (s)	0.075	0.1	0.075	0.0875
R (Hz/pu)	3	3.125	3.125	3.375
Control area parameters	Area 1		Area 2	
K_P (pu/Hz)	127.5		127.5	
T_P (s)	25		31.25	
B (pu/Hz)	0.532		0.495	

$$A = \begin{bmatrix}
\frac{-1}{T_{p1}} & 0 & \frac{K_{p1}}{T_{p1}} & \frac{K_{p1}}{T_{p1}} & 0 & 0 & 0 & 0 & \frac{-K_{p1}}{T_{p1}} \\
0 & \frac{-1}{T_{p2}} & 0 & 0 & \frac{K_{p2}}{T_{p2}} & \frac{K_{p2}}{T_{p2}} & 0 & 0 & \frac{K_{p2}}{T_{p2}} \\
\frac{-1}{2\pi \cdot R_1 \cdot (T_{g1}+T_{T1})} & 0 & \frac{-1}{(T_{g1}+T_{T1})} & 0 & 0 & 0 & \frac{-K_{i1} \cdot apf_1}{(T_{g1}+T_{T1})} & 0 & 0 \\
\frac{-1}{2\pi \cdot R_2 \cdot (T_{g2}+T_{T2})} & 0 & 0 & \frac{-1}{(T_{g2}+T_{T2})} & 0 & 0 & \frac{-K_{i1} \cdot apf_2}{(T_{g2}+T_{T2})} & 0 & 0 \\
0 & \frac{-1}{2\pi R_3 \cdot (T_{g3}+T_{T3})} & 0 & 0 & \frac{-1}{T_{g3}+T_{T3}} & 0 & 0 & \frac{-K_{i2} \cdot apf_3}{(T_{g3}+T_{T3})} & 0 \\
0 & \frac{-1}{2\pi R_4 \cdot (T_{g4}+T_{T4})} & 0 & 0 & 0 & \frac{-1}{T_{g4}+T_{T4}} & 0 & \frac{-K_{i2} \cdot apf_4}{(T_{g4}+T_{T4})} & 0 \\
\frac{B_1}{2 \cdot \pi} & 0 & 0 & 0 & 0 & 0 & 0 & 0 & 1 \\
0 & \frac{B_2}{2 \cdot \pi} & 0 & 0 & 0 & 0 & 0 & 0 & -1 \\
\frac{T_{12}}{2 \cdot \pi} & \frac{-T_{12}}{2 \cdot \pi} & 0 & 0 & 0 & 0 & 0 & 0 & 0
\end{bmatrix}_{9\times 9}$$

$$B = \begin{bmatrix}
\frac{-K_{p1}}{T_{p1}} & \frac{-K_{p1}}{T_{p1}} & 0 & 0 & \frac{-K_{p1}}{T_{p1}} & 0 \\
0 & 0 & \frac{-K_{p2}}{T_{p2}} & \frac{-K_{p2}}{T_{p2}} & 0 & \frac{-K_{p2}}{T_{p2}} \\
\frac{cpf_{11}}{T_{g1}+T_{T1}} & \frac{cpf_{12}}{T_{g1}+T_{T1}} & \frac{cpf_{13}}{T_{g1}+T_{T1}} & \frac{cpf_{14}}{T_{g1}+T_{T1}} & 0 & 0 \\
\frac{cpf_{21}}{T_{g2}+T_{T2}} & \frac{cpf_{22}}{T_{g2}+T_{T2}} & \frac{cpf_{23}}{T_{g2}+T_{T2}} & \frac{cpf_{24}}{T_{g2}+T_{T2}} & 0 & 0 \\
\frac{cpf_{31}}{T_{g3}+T_{T3}} & \frac{cpf_{32}}{T_{g3}+T_{T3}} & \frac{cpf_{33}}{T_{g3}+T_{T3}} & \frac{cpf_{34}}{T_{g3}+T_{T3}} & 0 & 0 \\
\frac{cpf_{41}}{T_{g4}+T_{T4}} & \frac{cpf_{42}}{T_{g3}+T_{T3}} & \frac{cpf_{43}}{T_{g4}+T_{T4}} & \frac{cpf_{44}}{T_{g4}+T_{T4}} & 0 & 0 \\
cpf_{31}+cpf_{41} & cpf_{32}+cpf_{42} & -(cpf_{13}+cpf_{23}) & -(cpf_{14}+cpf_{24}) & 0 & 0 \\
-(cpf_{31}+cpf_{41}) & -(cpf_{32}+cpf_{42}) & cpf_{13}+cpf_{23} & cpf_{14}+cpf_{24} & 0 & 0 \\
0 & 0 & 0 & 0 & 0 & 0
\end{bmatrix}_{9\times 6}$$

$$C = \begin{bmatrix}
1 & 0 & 0 & 0 & 0 & 0 & 0 & 0 & 0 \\
0 & 1 & 0 & 0 & 0 & 0 & 0 & 0 & 0 \\
0 & 0 & 1 & 0 & 0 & 0 & 0 & 0 & 0 \\
0 & 0 & 0 & 1 & 0 & 0 & 0 & 0 & 0 \\
0 & 0 & 0 & 0 & 1 & 0 & 0 & 0 & 0 \\
0 & 0 & 0 & 0 & 0 & 1 & 0 & 0 & 0 \\
0 & 0 & 0 & 0 & 0 & 0 & 1 & 0 & 0 \\
0 & 0 & 0 & 0 & 0 & 0 & 0 & 1 & 0 \\
0 & 0 & 0 & 0 & 0 & 0 & 0 & 0 & 1
\end{bmatrix}_{7\times 9}$$

References

[1] Kunder P. Power system stability and control. USA: McGraw-Hill; 1994.
[2] Jaleeli N et al. Understanding automatic generation control. IEEE Trans Power Syst 1992;7(3):1106–12.
[3] Vajk I, Vajta M, et al. Adaptive load–frequency control of the Hungarian power system. Automatica 1985;21(2):129–37.
[4] Kumar J, Ng Kah-Hoe, Sheble G. AGC simulator for price-based operation part 1: a model. IEEE Trans Power Syst 1997;12(2).
[5] Donde V, Pai A, Hiskens IA. Simulation and optimization in an AGC system after deregulation. IEEE Trans Power Syst 2001;16(3):481–9.
[6] Liu F, Song YH, Ma J, Mei S, Lu Q. Optimal load–frequency control in restructured power systems. IEE Proc Generat Transm Distribut 2003;150(1):87–95.
[7] Rerkpreedapong D, Feliachi A. Decentralized load frequency control for load following services. IEEE Power Eng Soc Winter Meet 2002;2(1):1252–7.
[8] Demiroren A, Zeynelgil HL. GA application to optimization of AGC in three-area power system after deregulation. Electr Power Energy Syst 2007;29(3):230–40.
[9] Bevrani H, Mitani Y, Tsuji K. Robust decentralized LFC design in a deregulated environment. Energy Convers Manage 2004;45:2297–312.
[10] Shayeghi H, Shayanfar HA, Malik OP. Multi-stage fuzzy PID power system automatic generation controller in deregulated environments. Energy Convers Manage 2006;47:2829–45.
[11] Lewis FL, Syrmos VL. Optimal control. Englewood Cliffs (New Jersey): Prentice Hall; 1995.
[12] Sedigh AK. Modern control systems. University of Tehran Press; 2003.
[13] MathWoks, Inc. Matlab. Control Toolbox, V.7.2; 2009.